Neural Computing and Applications (2019) 31:8859–8870
https://doi.org/10.1007/s00521-019-04422-3

ORIGINAL ARTICLE

Salp swarm algorithm-based model predictive controller for frequency regulation of solar integrated power system

Amita Singh[1] · Veena Sharma[1]

Received: 4 October 2018 / Accepted: 7 August 2019 / Published online: 23 August 2019

Abstract

Global analysis of power system markets project frequency regulation as one of the most profitable ancillary services. It is associated with second-to-second balance of load and frequency within a control area and acquires a principal role in enabling power interchanges while offering better conditions for electricity exchange. In the light of the above, a novel control strategy, namely salp swarm algorithm (SSA)-based model predictive controller, is proposed for frequency regulation of an unequal two-area realistic power system, incorporating solar thermal power plant and conventional thermal plant. Governor dead band, generation rate constraint and transport delay are considered in each control area. Over the past few years, model predictive controller (MPC) has come forward as a prediction-based control strategy for stabilizing dynamical systems while considering non-linearities, system uncertainties and constraints. The MPC parameters are optimized using SSA. The performance of the proposed approach is validated by comparing the dynamic time responses of SSA-optimized MPC with the other SSA-optimized conventional controllers, namely PID, FOPID and cascade PIDN-FOPID controller. The simulation result analysis shows that the proposed optimal MPC outpaces the conventional controllers with respect to peak overshoot, undershoot and settling time of the time responses. A comparative study of various objective functions indicates that, as compared to other indices, integral square error is better for the considered test system. Further, sensitivity analysis reveals the robustiousness of MPC parameters obtained at nominal values and hence is not required to be retuned, against variations in system loading and inertia constant.

Keywords Load frequency control (LFC) · Salp swarm algorithm (SSA) · Solar thermal power plant (STPP) · Model predictive controller (MPC) · Fractional-order proportional integral derivative (FOPID) · Integral square error (ISE)

List of symbols

f	Considered system frequency (Hz)
i	Referred subscript to area i, $i = 1, 2$
T_{12}	Synchronizing coefficient
ΔP_{Di}	Load variation in area i (p.u.)
T	Simulation time (s)
Δf_i	Frequency change in ith area (Hz)
D_i	$\Delta P_{Di}/\Delta f_i$ (p.u. MW/Hz)
K_{si}	Gain of solar field of ith area
B_i	Frequency bias constant of ith area
π	pi
K_{pi}	$1/D_i$ (Hz/p.u. MW)
H_i	Inertia constant of area i (s)
β_i	$(D_i + 1/R_i)$; area frequency response characteristics of ith area
R_i	Speed regulation parameter of governor of ith area (Hz/p.u. MW)
ΔP_{tie}	Incremental tie-line power deviation amid area 1 and area 2
T_{gi}	Time constant of steam governor for thermal power plant in ith area
K_{pfi}	Proportional gain of FOPID part of PIDN-FOPID cascade controller for ith area, $i = 1, 2$
μ_i	Order of differentiator of cascade PIDN-FOPID controller in ith area, $i = 1, 2$
T_{ti}	Time constant of steam turbine for thermal power plant in ith area
T_{gsi}	Time constant of steam governor for STPP in ith area
a_{12}	Area capacity ratio
T_{pi}	$2H_i/f/D_i$

✉ Amita Singh
amita@nith.ac.in

Veena Sharma
veena@nith.ac.in

[1] Electrical Engineering Department, National Institute of Technology Hamirpur, Hamirpur, Himachal Pradesh, India

T_o Working fluid outlet temperature of solar field (°C)
T_i Working fluid inlet temperature of solar field (°C)
T_e Environmental temperature (°C)
I Solar irradiance (W/m^2)
v Pump flow rate (m^3/s)
A Surface area of the collector
C Heat capacity of the working fluid (J/K)
η_0 Solar field collector efficiency
U_L Total heat loss coefficient (W/m^2 K)
T_{ri} Reheat steam turbine time constant of ith area (s)
K_{ri} Reheat coefficient of steam turbine of ith area
K_{pri} PID, FOPID, PIDN-FOPID proportional gain for ith area, $i = 1, 2$
K_{ini} PID, FOPID, PIDN-FOPID integral gain for ith area, $i = 1, 2$
K_{dei} PID, FOPID, PIDN-FOPID derivative gain for ith area, $i = 1, 2$
N_i PIDN-FOPID derivative filter coefficient for ith area, $i = 1, 2$
K_{dfi} Derivative gain of FOPID part of PIDN-FOPID cascade controller for ith area, $i = 1, 2$
K_{ifi} Integral gain of FOPID part of PIDN-FOPID cascade controller for ith area, $i = 1, 2$
λ_i Order of integrator of cascade PIDN-FOPID controller in ith area, $i = 1, 2$
T_{si} Solar collector time constant of ith area
T_{tsi} Time constant of steam turbine for STPP in ith area

1 Introduction

In a power system, watt and volt–ampere reactive power demands being dynamic, both frequency and voltage continuously change. The LFC, also termed as automatic generation control (AGC), controls the real power in an effort to keep a constant system frequency. The system frequency rests at its expected nominal value only when there is a balance between the real power generation and the real power demand, failing which the speed of the machine will fluctuate with subsequent deviation in system frequency [1]. These deviations must be detected, and the automatic control system must initiate control actions to counter these deviations, thus getting the power system back quickly to its original state. AGC uses the frequency deviations, and net real tie-line power interchanges between the neighbouring areas to evoke suitable valve actions of generators in reaction to system load fluctuations. Thus, the key objectives of the AGC are: (1) to hold the frequency of the system at or very close to a stated theoretical value and (2) to keep up the scheduled net interchanges of real power amongst the control areas [2].

From the already existing work, it can be observed that a wide and extensive research has been done on AGC of interconnected power systems [3–7]. An extensive and exhaustive bibliographic survey on classical and optimal control strategies, linear and nonlinear power system models, AGC strategies based on digital, soft computing, self-tuning control and adaptive control have been presented by Ibraheem et al. [3]. Analysis on challenges in LFC integrating storage devices such as battery energy storage system (BESS), wind–diesel system, PV systems and FACTS devices was presented by Pandey et al. [4]. Janardan Nanda et al. [5] studied the generation control of a two-area interconnected thermal–hydro power system applying classical controllers, while considering system non-linearities. Researchers in [6] have put forward a comprehensive dynamic analysis of a more realistic power system under deregulated environment with varied sources such as hydro, thermal and gas in each control area. In 2012, Das et al. [7] researched the models of an isolated hybrid generation system such as wind, diesel, aqua electrolysers, photovoltaic, STPP, flywheel, BESS, fuel cells and ultra-capacitors.

Owing to the price of conventional sources of power and the grave environmental problems, the usage of non-conventional energy sources, particularly the solar energy, is continuously increasing [8]. The modelling and concepts of combining solar power in a multi-source power plant have been presented in the literature [9–12]. Buzas et al. [9] proposed a validated solar collector transfer function based on a mathematical model, already present in the literature, that can be easily employed for the control design and dynamical analysis. Based on the solar collector transfer function model proposed by Buzas in [9], Sharma et al. [10] presented the frequency control of an interconnected unequal two-area system integrating STPP and thermal plant, using grey wolf optimization (GWO)-optimized PID controller. Researchers in [11] studied the effect of using ultra-capacitors on load frequency regulation of a two-area STPP–thermal power plant using recent PIDN-FOPID controller under deregulated environment. The concept of an integrated multi-source model of automatic voltage regulator and LFC in a STPP–thermal power plant, using lightning search algorithm (LSA), was addressed by Rajbongshi et al. [12].

The AGC action is predominantly divided into a primary control action and a secondary control action. In case of a sudden increase in electrical load on a generator, the deviation in frequency is compensated by the speed governor action called the primary control. However, in case of mismatch over few seconds to several minutes, the frequency cannot be maintained at a constant value by

employing the speed governor action alone. Hence, the sudden load variations are minimized while maintaining the system frequency at nominal value by exercising a secondary control mechanism in the form of controllers. Currently, for a reliable operation of power system, nearly all the investigation on AGC is targeted on design of efficient and improved controllers [11, 13–18]. Various controllers, namely integral (I), proportional integral (PI), integral derivative (ID), proportional integral derivative (PID) [13, 14], integral double derivative (IDD) [13], parallel 2-degree-of-freedom proportional integral derivative (2-DOF PID) [15], modern controllers like FOPID [16], model predictive controller (MPC) [17], cascaded controllers [11], intelligent and advanced controllers like artificial neural network (ANN) and fuzzy logic controller (FLC) [14, 18] controllers, have been discussed in the above literature. These control schemes deliver good dynamic response and reduce the deviations in the system as well as the steady-state error in tie-line real power flow and fluctuations in system frequency. The setback for conventional or classical controllers over modern controllers is their lack of efficacy in handling system nonlinearities and constraints as well as their gradual transient response. The implementation of MPC is not yet considered in interconnected multi-area systems incorporating renewable sources like solar thermal power plant.

The power system performance mostly depends on the gains and parameters of the controller; thus, they must be optimally tuned using good and efficient optimization approaches. Nowadays, engineers dedicated in power sector have used various optimization approaches, namely genetic algorithm (GA), gravitational search algorithm (GSA) and its different variants [19], firefly algorithm (FFA) [10, 20], particle swarm optimization (PSO) [11] and cuckoo search algorithm (CSA) [12] for LFC under both conventional and deregulated environments. Recently, GWO [21, 22], ant lion optimization (ALO) [23, 24], whale optimization algorithm (WOA) [25], grasshopper optimization algorithm (GOA) [26], LSA [12] and SSA [27] have been developed. Amongst the methods, PSO is the pioneer one and SSA is the most recently developed optimization algorithm. GA requires a large number of objective function evaluations with lengthy computation time especially for large dimensional problems [28]. Like GA, PSO also has a disadvantage of getting trapped in local optimum solution. The performance of any technique mainly depends on the balance between exploitation and exploration mechanisms [29]. With poor exploration capability, algorithms such as bat algorithm [30] easily get trapped into the local minima, whereas GWO and artificial bee colony (ABC) show a much better performance, especially on the functions with a large number of local minima. CSA and FFA do not perform as well as GWO and ABC in terms of convergence rate and search efficiency and need more iterations to reach the global optima [28]. The authors [31] presented the superiority of GWO over differential evolution (DE), PSO and ABC approaches. The main advantages of the GWO method include quick convergence, more accurate results and highly robust and strong exploration ability over the search space. The advantages of WOA over PSO and FFA were shown by Saha et al. [11]. Recently, another swarm-based algorithm has been introduced by Mirjalili et al. [27] in 2017. The authors [27] presented the effectiveness of SSA over DE, PSO and GSA by conducting experiments on 19 different benchmark functions.

SSA is inspired by the swarming attitude of salps, while navigating and searching in oceans. Also, it employs an adaptive mechanism to balance convergence and divergence. Thus, this technique is able to approach the global optimum solution of day-to-day world single- and multi-objective problems with inspiring and unfamiliar investigating areas. However, the SSA approach is not yet applied for optimal tuning of parameters and gains of controllers in LFC of STPP–thermal power plants under conventional and deregulated environments.

Thus, in consideration of the above, the main objectives of the present work are listed below:

(a) To design a load frequency model of an unequal two-area STPP–thermal power plant with appropriate governor dead band (GDB) and generation rate constraint (GRC).
(b) To optimally tune the gains and parameters of PID, FOPID, PIDN-FOPID cascade controllers, as well as output signal weight, manipulated variable weight and manipulated variable rate weight parameters of MPC using salp swarm algorithm (SSA). Further, using the above-mentioned controllers the dynamic time response of the system considered in (a) is obtained.
(c) To perform a comparative analysis of dynamic time responses of the considered system while applying the controllers mentioned above, in order to find the most suitable controller for the considered system.
(d) To evaluate the different objective functions used for optimal tuning using SSA, so as to attain the best suitable objective function for the system considered in (a).
(e) To carry out sensitivity analysis for efficiency and robustness of the proposed SSA-optimized MPC controller.

2 Test system

The system investigated in this paper is an unequal two-area interconnected STPP–thermal power plant with area capacity ratio of area 1 to area 2 = 2:5. Each control area consists of a STPP and a fuel unit comprising of single reheat turbine. Non-linearities such as GDB of 0.06% (0.036 Hz) and GRC of 3%/min with each reheat thermal unit make the considered system more realistic in nature. To study the system dynamics, a 0.01 p.u. step load perturbation is considered as disturbance in area 1. For each control area, the considered parameters for thermal system are obtained from [13] and the considered parameters for solar thermal power plant are obtained from [7, 10]. PID, FOPID, PIDN-FOPID cascade controller and MPC are considered for the necessary secondary control action. The controller parameters, gains and filter coefficient are optimized using a novel meta-heuristic optimization approach named as SSA. The Simulink transfer function block diagram model of the considered system is presented in Fig. 1. The different cost functions considered for the investigation are: integral squared error (ISE), integral absolute error (IAE), integral time square error (ITSE) and integral time absolute error (ITAE), shown by Eqs. (1–4), respectively

$$J_1 = \int_0^T \left\{ (\Delta f_i)^2 + (\Delta P_{\text{tie}})^2 \right\} \mathrm{d}t \tag{1}$$

$$J_2 = \int_0^T \{ |\Delta f_i| + |\Delta P_{\text{tie}}| \} \mathrm{d}t \tag{2}$$

$$J_3 = \int_0^T \left\{ (\Delta f_i)^2 + (\Delta P_{\text{tie}})^2 \right\} t \mathrm{d}t \tag{3}$$

$$J_4 = \int_0^T \{ |\Delta f_i| + |\Delta P_{\text{tie}}| \} t \mathrm{d}t \tag{4}$$

where i denotes the number of control areas =1, 2 and T is the simulation time in seconds. The turbine, reheat turbine and governor transfer function are represented by Eqs. (5–7), respectively

$$G_{ti}(s) = \frac{1}{1 + sT_{ti}} \tag{5}$$

$$G_{rti}(s) = \frac{1 + sK_{ri}T_{ri}}{1 + sT_{ri}} \tag{6}$$

$$G_{gi}(s) = \frac{1}{1 + sT_{gi}} \tag{7}$$

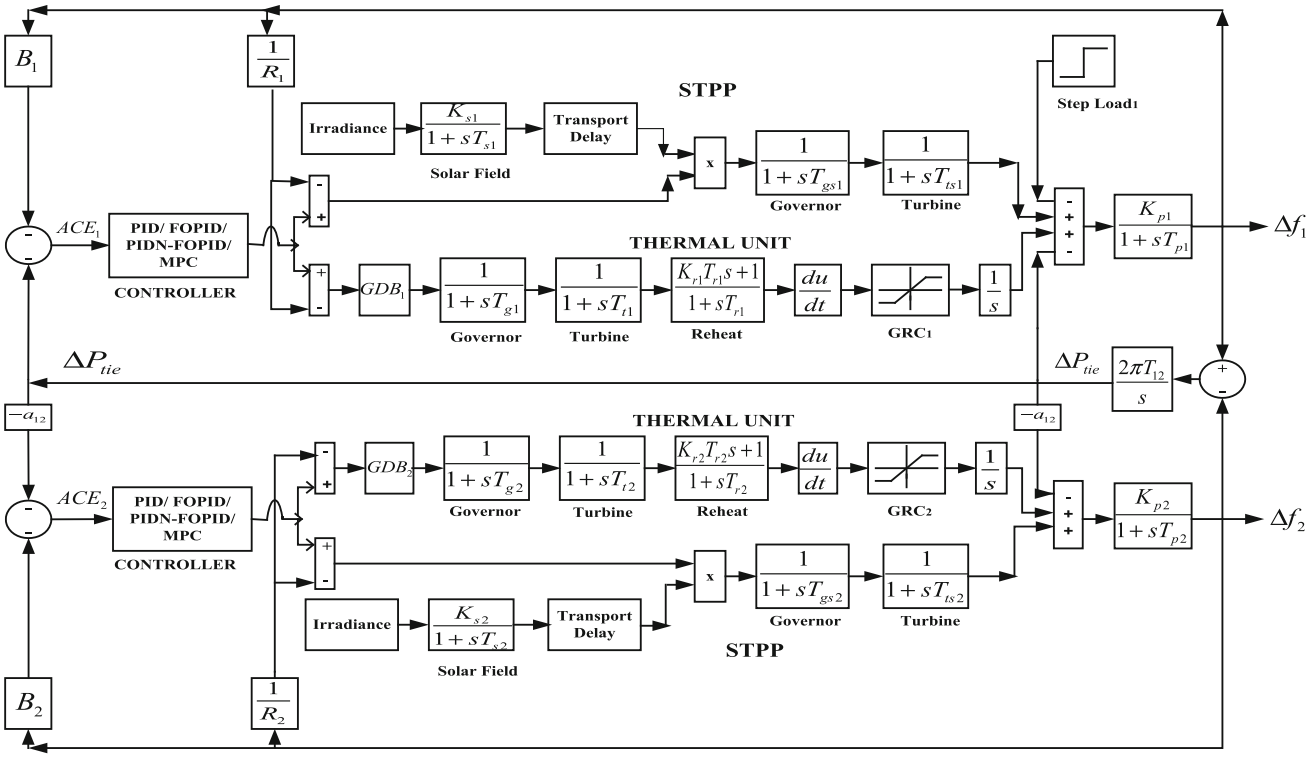

Fig. 1 Simulink transfer function block diagram model of STPP–thermal power system

Similarly, the solar field transfer function is presented by [9], as shown below

$$G_i(s) = \frac{K_{si}}{1 + sT_{si}} \tag{8}$$

where T_{si} denotes the solar collector time constant and is represented as $T_{si} = \frac{1}{\left(\frac{U_L A}{2C} + \frac{v}{V}\right)}$, where V denotes volume of the heat transfer fluid present in the collector (m^3). For the different processes of STPP, a transport delay of 1 s is considered in each area of the system [9].

3 Model predictive controller (MPC)

Model predictive controller has been presented as a novel method for automatic generation control of power systems incorporating non-conventional energy sources such as STPP. MPC is a prediction-based control technique where, at every sampling interval, an optimum control action is attained over a predefined prediction range. It presents many advantages, like robustness, quick response and stability against system uncertainties and non-linearities [32]. The controller action relies on a prespecified number of prediction and control moves across both manipulated and controlled variable measurements. MPC designer can preassign the sampling interval. The control estimates rely on both predicted future output values and current obtained output values. Figure 2 presents the elementary conceptual diagram representing MPC [33]. The primary goal of MPC is to compute a sequence of control moves in the manipulated variable, in such a way that the system can be optimally tracked to its set or reference value [17]. The MPC state space representation is expressed by the following equations:

$$x(k+1) = \phi x(k) + \tau_v v(k) \tag{9}$$

$$y(k) = \hat{y}(k) \tag{10}$$

$$y(k) = Cx(k) + D_u u(k) + D_v v(k) \tag{11}$$

where a vector of n state variables is represented by x and u denotes manipulated variables present in the system and also enacts as an actuator. v typifies measured disturbances, whereas constant matrices are symbolized by ϕ and τ_v. $\hat{y}$ denotes the predicted output of the considered plant. C, D_u and D_v are constant matrices [34]. MPCobj = mpc(Plant, T_s, P, M, W) creates an object based on a plant model, sampling interval (T_s), prediction horizon (P), control horizon (M), output, manipulated variable and manipulated variable rate weights (W). All the parameters stating the MPC control law are stored in an MPC object.

MPC as a modern control approach obtains the solution for an optimization problem with the help of an objective function, for every time instant k, based on predicted future output values across a prediction range of P time steps. The objective function minimization is achieved by selecting manipulated variable moves, over a M-move control range. Despite the fact that at each time step a set of M moves is computed, only the first move $u(k+1)$ is put into effect. Following the realization of this step, the results $y(k+1)$ at the next successive time step is attained. These courses of actions are conducted for every k time step [35]. The foremost aim of MPC is to bring down the output error to zero. The objective function J, which is to be minimized, is in general a weighted sum of square of predicted future

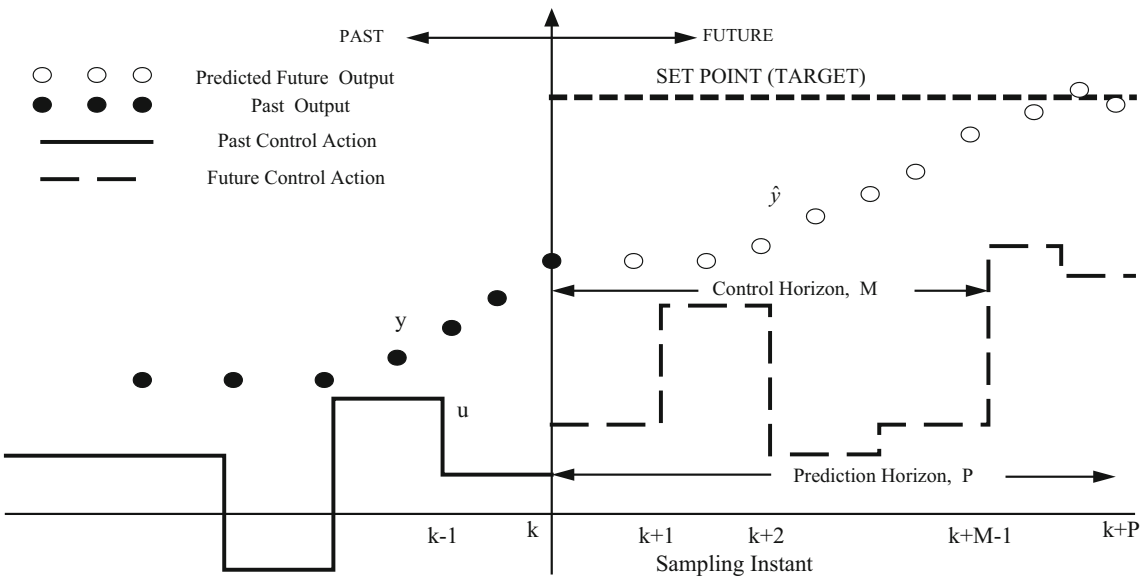

Fig. 2 Basic conceptual diagram representing model predictive controller [33]

errors and square of future control output values, as represented by the equation shown below

$$J(N_1,N_2,N_u)=\sum_{j=N_1}^{N_2}\beta(j)[\hat{y}(k+j|k)-w(k+j)]^2+\sum_{j=1}^{N_u}\lambda(j)[u(k+j-1)]^2 \quad (12)$$

where N_1 and N_2 denote the lower bound and upper bound prediction ranges over the output, respectively, the control limit is represented by N_u, the weighting factors are denoted by $\beta(j)$ and $\lambda(j)$, whereas the trajectory of reference line across the future bound N is denoted by $w(k+j)$. Herein, measured disturbance of 0.01 p.u. MW is considered in area 1 of the test system and unmeasured disturbances are supposed to be absent. In this work, the MPC parameters considered for tuning are manipulated variable weights (u_i), output signal weights (y_i) and manipulated variable rate weights (du_i) [35]. The above-stated MPC parameters are tuned using SSA so as to minimize the objective functions (Eqs. 1–4), subject to the following constraints [32]

$$\begin{aligned} u_i^{\min}\le u_i\le u_i^{\max}\\ y_i^{\min}\le y_i\le y_i^{\max}\\ du_i^{\min}\le du_i\le du_i^{\max}\end{aligned} \quad (13)$$

within the limits of 0 and 1. $u_i^{\min}$, $y_i^{\min}$, $du_i^{\min}$ and $u_i^{\max}$, $y_i^{\max}$, $du_i^{\max}$ are lower and upper bounds of MPC parameters, respectively.

4 Salp swarm algorithm (SSA)

A novel meta-heuristic optimization technique called SSA is presented in this work for optimal tuning of different controller gains, parameters and filter coefficient. In 2017, Seyedali Mirjalili et al. proposed a recent swarm intelligence optimizer named SSA. It is nature-inspired population-based algorithm that follows the floating behaviour of salps, in the form of salp chains while navigating in oceans and seas. SSA saves and assigns the best solution obtained so far to the food source variable, so it never gets lost even if the whole population declines. It outperforms many algorithms such as GA, PSO, GSA, CSA and FF due to its adaptive nature, high exploration and exploitation using the converging and diverging parameter, minimum feature selection and hence less execution time and better accuracy of results. Many stochastic operators incorporated into SSA let this technique to be better than many approaches and prevent them from being trapped at local optimal solutions in multi-modal search spaces [27].

The algorithm starts with dividing the random population into two classes: the leader and the followers. The salp positioned at the very start of the salp chain is regarded as the leader, while the salps other than the leader salp are considered as follower salps. The leader salp being the best solution directs the swarm of salps, whereas the follower salps follow each other. The position of the leader is updated using the following equations

$$x_j^1=F_j+c_1\left(\left(ub_j-lb_j\right)c_2+lb_j\right)\quad c_3\ge 0 \quad (14)$$

$$x_j^1=F_j-c_1\left(\left(ub_j-lb_j\right)c_2+lb_j\right)\quad c_3\le 0 \quad (15)$$

where x_j^1 represents the position of leader and F_j represents the food source position in dimension j. ub_j and lb_j are the maximum and minimum limits in dimension j, respectively. c_1, c_2 and c_3 are random numbers, where c_2 and c_3 are uniformly created random numbers. Coefficient c_1 balances convergence and divergence, expressed as below:

$$c_1=2e^{-\left(\frac{4l}{L}\right)^2} \quad (16)$$

where l denotes the current and L denotes the maximum number of epochs. The position of the follower salps is revised using the below equation

$$x_j^i=\frac{1}{2}\left(x_j^i+x_j^{i-1}\right);\quad i\ge 2 \quad (17)$$

where x_j^i depicts the location of ith salp follower in dimension j [27]. The leader salp revises its location depending upon the source of food or the fittest solution. The rest of the salps (followers) follow the food source and update their positions accordingly. The process continues until the fittest solution is obtained or a stopping criterion is met. The pseudocode and flowchart of SSA is presented in Figs. 3 and 4, respectively.

The tuned values of input parameters applied in SSA are: number of search agents (NP) = 30 and maximum number of iterations = 50. The output variables in this paper are the values of parameters and gains of controllers. The output variables of PID controller is given as

```
Initialize the population of salps x_i (i = 1, 2, .., n) considering lb and ub
  while (stopping criteria is not met)
  Calculate the fitness value of each salp
   Set F as the best salp
  Update the parameter c_1 using Eq. (16)
    for salp x_i
        if (i==1)
            Update the position of leader salp by Eq. (14) and Eq. (15)
        else
            Update the position of follower salps by Eq. (17)
        end
    end
  Update the position of salps considering lower and upper limits of variables
end
return F
```

Fig. 3 Pseudocode of salp swarm algorithm

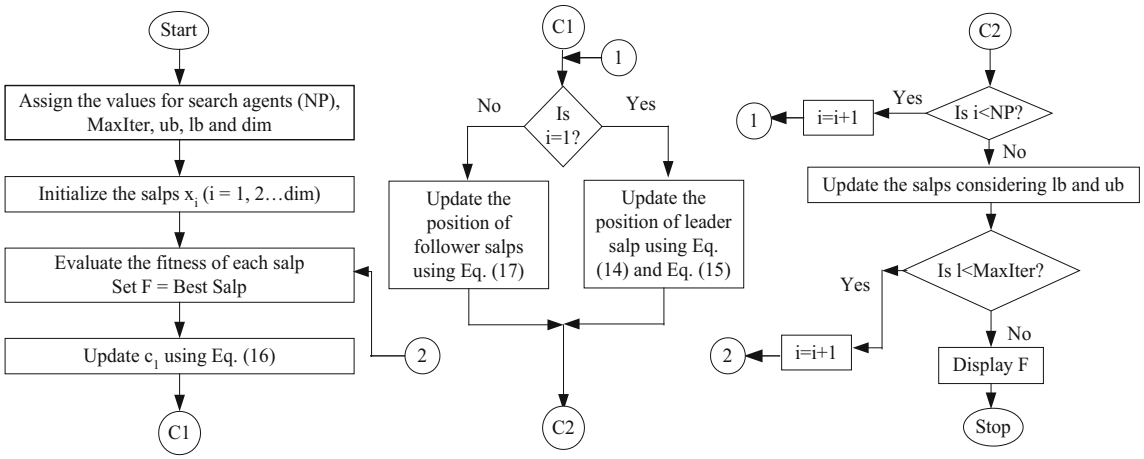

Fig. 4 Flowchart of salp swarm algorithm

$$[K_{pr1}K_{pr2}K_{in1}K_{in2}K_{de1}K_{de2}] \tag{18}$$

The output variables of FOPID controller is given as

$$\left[K_{pr1}K_{pr2}K_{in1}K_{in2}K_{de1}K_{de2}\mu_1\mu_2\lambda_1\lambda_2\right] \tag{19}$$

The output variables of PIDN-FOPID controller is given as

$$\begin{aligned}&\left[K_{pr1}K_{pr2}K_{in1}K_{in2}K_{de1}K_{de2}N_1N_2K_{pf1}\right.\\&\left.K_{pf2}K_{if1}K_{if2}K_{df1}K_{df2}\mu_1\mu_2\lambda_1\lambda_2\right]\end{aligned} \tag{20}$$

The output variables of MPC is given as

$$[u_1u_2y_1y_2du_1du_2] \tag{21}$$

In this work, the variables range between 0 and 1 excluding N_i, i= 1, 2, for which the range taken into consideration is between 0 and 100. The considered bound of frequency for Oustaloup approximation is [0.01, 50] [11].

5 Results and analysis

5.1 Comparison of MPC with conventional controllers

Here, MPC as well as conventional controllers such as PID, FOPID and cascade PIDN-FOPID are used as secondary control for lowering frequency deviations, area control error (ACE) and controlling the variations in real power flow of the considered power system. These controllers are used independently, in each control area. MPC toolbox in MATLAB/Simulink environment on MATLAB 2018 has been used to design the MPC. In this work, considered MPC parameters are prediction horizon (P) = 13; control horizon (M) = 2; sampling interval = 0.0002 s [32]. In each case, system responses are attained by taking into account a 1% step load perturbation as disturbance, in area 1 of the system under investigation. An error band of 0.1% is considered while calculating steady-state error and settling time.

For each controller, the tunable parameters and gains are simultaneously optimized exercising SSA technique. The SSA-optimized values of controller gains, order of integrator and differentiator and filter coefficient are presented in Table 1. Using the attained optimum values, the dynamic response of each controller is obtained and assessed. The time-domain simulation responses of SSA-optimized MPC, PIDN-FOPID cascade, FOPID and PID in the form of frequency deviation in area 1 and area 2, tie-line real power deviation and area control error are shown in Fig. 5. Based on dynamic time responses, the performance attributes such as settling time, peak undershoot and peak overshoot, as given in Table 2, show that there is an improvement of 62.79%, 44.03% and 34.33% in settling time with MPC as compared to PID, FOPID and PIDN-FOPID cascade controller, respectively, in frequency deviation in area 1. Also, there is an improvement of 58.96%, 35.38% and 31.61% in settling time with MPC as for PID, FOPID and PIDN-FOPID cascade controller, respectively, in net tie-line power deviation. Therefore, Fig. 5 and Table 2 show that SSA-optimized MPC control strategy outperforms the other conventional controllers in terms of settling time, peak undershoot and overshoot.

The performance of SSA technique is evaluated by comparing its dynamic behaviour with GWO, WOA, GOA and PSO, while considering same population size and maximum number of iterations for the above-studied test power system. Using the above-mentioned optimization techniques, the controller gains and parameters are optimized simultaneously, one controller at a time. Figure 6 presents the dynamic time responses corresponding to the optimized parameters of MPC using SSA, WOA, GWO, GOA and PSO techniques. In Fig. 6, the responses of SSA, WOA, GWO, GOA and PSO techniques in terms of

Table 1 Optimum values of parameters and gains for different controllers in nominal condition

Controller	Control area	Optimal values of parameters				
PID	Area 1	$K_{pr1} = 0.9993$	$K_{in1} = 0.8275$	$K_{de1} = 0.6982$		
FOPID	Area 2	$K_{pr2} = 0.9991$	$K_{in2} = 0.4321$	$K_{de2} = 0.8321$		
	Area 1	$K_{pr1} = 0.7789$	$K_{in1} = 0.3425$	$K_{de1} = 0.9884$	$\mu_1 = 0.9971$	$\lambda_1 = 0.8992$
	Area 2	$K_{pr2} = 0.8318$	$K_{in2} = 0.8955$	$K_{de2} = 0.9680$	$\mu_2 = 0.9994$	$\lambda_2 = 0.4936$
PIDN-FOPID cascade	Area 1	$K_{pr1} = 0.9813$	$K_{in1} = 0.3820$	$K_{de1} = 0.0198$	$N_1 = 4.6213$	$K_{pf1} = 0.5953$
		$K_{if1} = 0.0026$	$K_{df1} = 0.9984$	$\mu_1 = 0.7218$	$\lambda_1 = 0.4252$	
	Area 2	$K_{pr2} = 0.9854$	$K_{in2} = 0.0034$	$K_{de2} = 0.9946$	$N_2 = 6.9974$	$K_{pf2} = 0.9709$
		$K_{if2} = 0.6010$	$K_{df2} = 0.9970$	$\mu_2 = 0.4359$	$\lambda_2 = 0.9443$	
MPC	Area 1	$u_1 = 0.3150$	$y_1 = 0.9975$	$du_1 = 0.0102$		
	Area 2	$u_2 = 0.5089$	$y_2 = 0.8994$	$du_2 = 0.0056$		

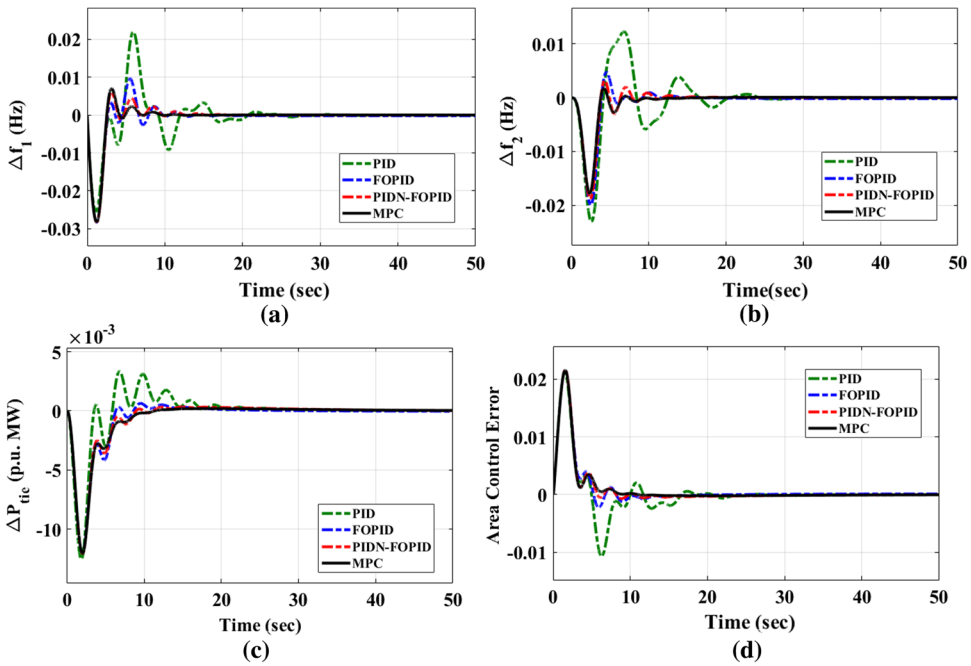

Fig. 5 Dynamic response comparison of SSA-optimized controllers: **a** frequency deviation in area 1 with respect to time, **b** frequency deviation in area 2 with respect to time, **c** net tie-line power flow deviation with respect to time, **d** ACE in area 1 versus time

Table 2 Dynamic response comparison with respect to settling time (s), peak undershoot and peak overshoot

Figures	Parameters		PID	FOPID	PIDN-FOPID	MPC
Figure 5a	Δf_1	Settling time (s)	32.430	21.553	18.370	12.064
		Peak undershoot	− 0.02551	− 0.02832	− 0.02827	− 0.02824
		Peak overshoot	0.02202	0.03339	0.05996	0.006377
Figure 5b	Δf_2	Settling time (s)	34.772	17.779	16.731	12.367
		Peak undershoot	− 0.02307	− 0.01997	− 0.01883	− 0.01735
		Peak overshoot	0.01230	0.004791	0.003173	0.001782
Figure 5c	ΔP_{tie}	Settling time (s)	35.960	22.837	21.576	14.756
		Peak undershoot	− 0.01254	− 0.012081	− 0.012092	− 0.01207
		Peak overshoot	0.0005379	0.0003467	0.001621	0.0002008
Figure 5d	ACE_1	Settling time (s)	32.095	19.001	17.837	11.668
		Peak undershoot	− 0.01073	− 0.002276	− 0.0007240	− 0.0002118
		Peak overshoot	0.02114	0.02167	0.02167	0.02161

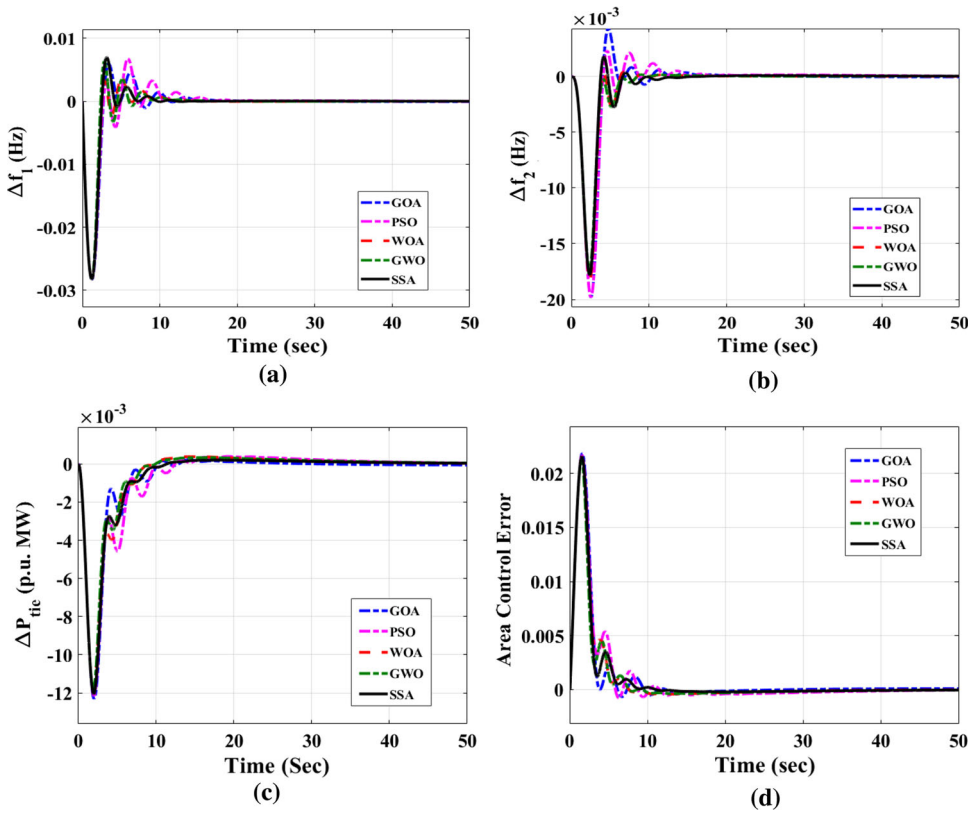

Fig. 6 Dynamic response comparison of different algorithm-optimized MPCs: **a** frequency deviation in area 1 with respect to time, **b** frequency deviation in area 2 with respect to time, **c** net tie-line power flow deviation with respect to time, **d** ACE in area 1 versus time

attributes such as frequency variation in area 1, frequency variation in area 2 and net tie-line active power flow deviation are compared. It can be observed that SSA-optimized MPC performs better than WOA, GWO, GOA and PSO-optimized MPC, as SSA-based MPC has faster settling time and lesser peak over and undershoot. Also, the convergence curve of SSA, GWO, WOA, GOA and PSO techniques is presented in Fig. 7. Figure 7 shows that SSA converges at a faster rate than WOA, GWO, GOA and PSO. Convergence depends upon the complexity, computational burden, memory requirement and hence on the number of parameters required to be adjusted in an algorithm. SSA has only one controlling parameter (c_1), PSO has three parameters (inertial weight, personal influence factor and social influence factor), whereas, GOA, WOA and GWO each have two controlling parameters. Therefore, SSA requires less memory storage and can be easily implemented. Moreover, steady movement of follower salps prevent the algorithm from being trapped easily in local optima [27].

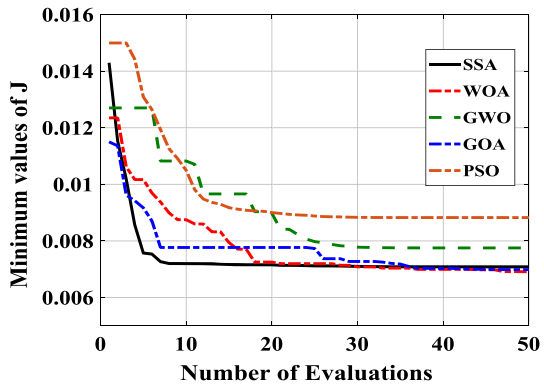

Fig. 7 Convergence curve of different optimization algorithms

Table 3 Objective functions and optimum values of MPC parameters for different objective functions

Objective function	Value	Optimal values of MPC parameters	
		Area 1	Area 2
ISE	0.0015	$u_1 = 0.2144$	$u_2 = 0.7540$
		$y_1 = 0.9938$	$y_2 = 0.9733$
		$du_1 = 0.1782$	$du_2 = 0.0631$
IAE	0.1276	$u_1 = 0.1502$	$u_2 = 0.0119$
		$y_1 = 0.9815$	$y_2 = 0.9464$
		$du_1 = 0.0175$	$du_2 = 0.1276$
ITSE	0.0028	$u_1 = 0.2580$	$u_2 = 0.1354$
		$y_1 = 0.9889$	$y_2 = 0.9775$
		$du_1 = 0.00931$	$du_2 = 0.0298$
ITAE	0.5526	$u_1 = 0.4039$	$u_2 = 0.5467$
		$y_1 = 0.9584$	$y_2 = 0.9945$
		$du_1 = 0.0585$	$du_2 = 0.0101$

5.2 Objective function (J) selection

In this paper, different cost functions or objective functions such as IAE, ISE, ITAE and ITSE are addressed. Each cost function is considered one at a time for the system under study, and in every case, the parameters of MPC are optimally tuned using SSA. The resultant optimum values of MPC parameters and objective functions are presented in Table 3. The dynamic time responses corresponding to each performance index in terms of deviation in frequency in area 1 and tie-line real power flow are presented in Fig. 8. The values of objective function in Table 3 show that integral squared error (ISE) has least value and hence minimum error as compared to other performance indices. Also Fig. 8 shows that ISE has better response in terms of peak deviations and settling time as compared to others. Hence, ISE is qualifying as the performance index for the test system under study.

5.3 Sensitivity analysis

A sensitivity analysis is performed on SSA-optimized MPC parameters, achieved at nominal condition, to evaluate the robustiousness and efficiency of the proposed control scheme for considered power systems under wide fluctuations in inertia constant and loading condition. Herein, loading condition and inertia constant are varied in the range of ± 25% of the given nominal or assumed values. For every case, the parameters and controller gains are optimized independently employing SSA. The simulation time response obtained at each varied condition with respect to their corresponding optimally tuned value of parameters is evaluated with that obtained at nominal case and is presented in Fig. 9. Figure 9 shows that the response at varied condition is almost same as that of nominal condition. Hence, it can be concluded that SSA-optimized MPC parameters are vigorous and therefore need not be

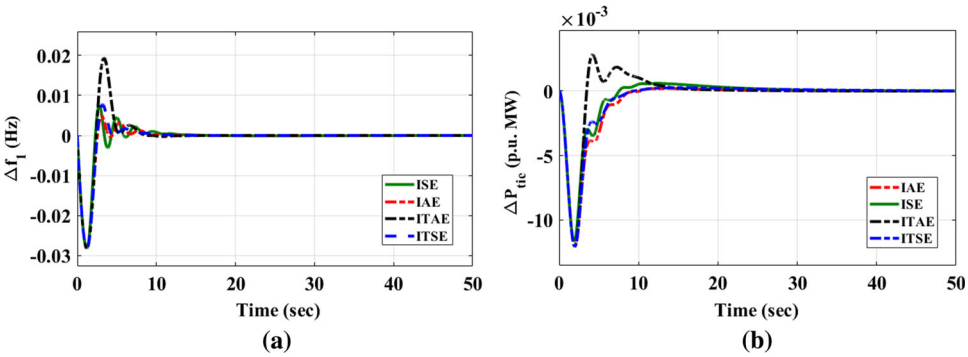

Fig. 8 Dynamic response comparison of different objective functions with MPC controller: **a** deviation in frequency in area 1 with respect to time, **b** net deviation in tie-line power flow with respect to time

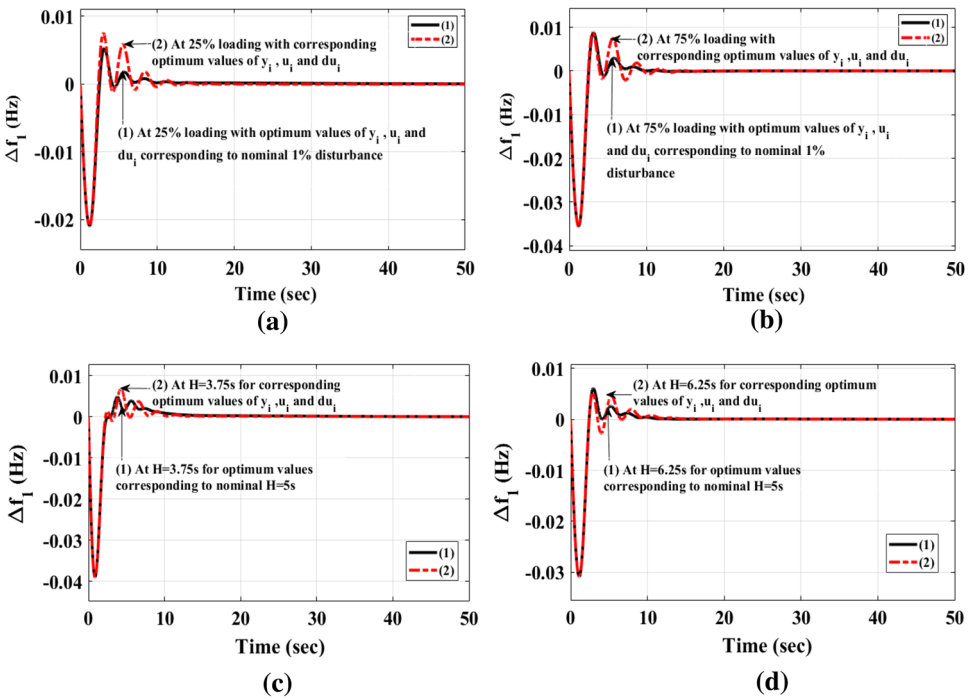

Fig. 9 Dynamic response comparison for frequency deviation in area 1: **a** frequency deviation in area 1 with respect to time for 25% loading, **b** frequency deviation in area 1 with respect to time for 75% loading, **c** frequency deviation in area 1 with respect to time for $H = 3.75$ s, **d** frequency deviation in area 1 with respect to time for $H = 6.25$ s

retuned when subjected to variations in inertia constant and loading condition.

6 Conclusions

In this work, an effort has been made to implement model predictive controller as a secondary control for frequency regulation of an unequal two-area interconnected power system incorporating solar thermal power plant as a non-conventional source and a thermal power plant. A new optimization approach called SSA has been effectively applied for optimal tuning of model predictive controller parameters as well as gains of various conventional controllers. The robustiousness of proposed control strategy is evaluated from its dynamic behaviour in time-domain simulations of the power system taken under investigation. The dynamic behaviour of the considered system, studied in terms of peak undershoot, peak overshoot and settling time, exhibits that the functioning of the SSA-optimized MPC outperforms the performance of conventional controllers in minimizing the ACE and augmenting the performance of the considered system. Also, SSA-based MPC control scheme is capable of handling non-linearities existing in a realistic interconnected power system. Investigations on the choice of objective function explored that ISE is more suitable for the considered test system. The sensitivity analysis performed on SSA-optimized MPC parameters, subject to wide fluctuations in system loading conditions and inertia constant parameter, presents the robust nature of the controller parameters and hence needs not to be reset again and again in case of large inertia constant and system loading variations.

Acknowledgements This research work is sponsored by the Council of Scientific & Industrial Research, New Delhi, India, under the Research and Development Project Grant 22(0692)/15/EMR-II.

Compliance with ethical standards

Conflict of interest The authors declare that they have no conflict of interest.

Appendix

Nominal parameters considered for the test system are [7, 10, 13]: $f = 60$ Hz; 1% step load disturbance in area 1; $T_{ts} = 3.0$ s; $T_{gs} = 1.0$ s; $T_{g1} = 0.08$ s, $T_{g2} = 0.08$ s; $T_{t1} = 0.3$ s, $T_{t2} = 0.3$ s; $K_{ri} = 0.5$ s; $T_{ri} = 10$ s; $T_{pi} = 20$ s; $K_{pi} = 120$ Hz/p.u. MW; $T_{12} = 0.08$ p.u. MW/rad; $D_i = 8.33 \times 10^{-3}$ p.u. MW/Hz; $R_i = 2.4$ Hz/p.u. MW; $B_i = 0.425$ p.u. MW/Hz; $H_i = 5$ s; $T_s = 1.8$ s; $K_s = 1.8$.

References

1. Sivanagaraju S, Sreenivasan G (2017) Power system operation and control, 255–362, 19th edn. Pearson, India
2. Uma Rao K (2016) Power system operation & control, 185–294, 3rd edn. Wiley, India
3. Ibraheem, Kumar P, Kothari DP (2005) Recent philosophies of automatic generation control strategies in power systems. IEEE Trans Power Syst 20(1):346–357
4. Pandey SK, Mohanty SR, Kishor N (2013) A literature survey on load–frequency control for conventional and distribution generation power systems. Renew Sust Energy Rev 25:318–334
5. Nanda J, Mangla A, Suri S (2006) Some new findings on automatic generation control of an interconnected hydrothermal system with conventional controllers. IEEE Trans Energy Convers 21:187–194
6. Hota PK, Mohanty B (2016) Automatic generation control of multi-source power generation under deregulated environment. Int J Electr Power Energy Syst 75:205–214
7. Das DCh, Roy AK, Sinha N (2012) GA based frequency controller for solar thermal–diesel–wind hybrid energy generation/energy storage system. Electr Power Energy Syst 43:262–279
8. Bevrani H, Ghosh A, Ledwich G (2010) Renewable energy sources and frequency regulation: survey and new perspectives. IET Renew Power Gener 4(5):438–457
9. Buzas J, Kicsiny R (2014) Transfer functions of solar collectors for dynamical analysis and control design. Renew Energy 68:146–155
10. Sharma Y, Saikia LC (2015) Automatic generation control of a multi-area ST–thermal power system using Grey Wolf optimizer algorithm based classical controllers. Int J Electr Power Energy Syst 73:853–862
11. Saha A, Saikia LC (2017) Utilisation of ultra-capacitor in load frequency control under restructured STPP-thermal power systems using WOA optimised PIDN-FOPD controller. IET Gener Transm Distrib 11(13):3318–3331
12. Rajbongshi R, Saikia LC (2017) Combined control of voltage and frequency of multi-area multisource system incorporating solar thermal power plant using LSA optimised classical controllers. IET Gener Transm Distrib 11(10):2489–2498
13. Chandra Saikia Lalit, Nanda J, Mishra S (2011) Performance comparison of several classical controllers in AGC for multi area interconnected thermal system. Int J Electr Power Energy Syst 33(3):394–401
14. V. Shanmuga Sundaram, T. Jayabarathi (2011) Load frequency control using PID tuned ANN controller in power system. In: 1st international conference on electrical energy systems, pp 269–274
15. Kumar Sahu Rabindra, Sidhartha Panda, Kumar Rout Umesh (2013) DE optimized parallel 2-DOF PID controller for load frequency control of power system with governor dead-band nonlinearity. Electr Power Energy Syst 49:19–33
16. Dahiya P, Sharma V, Naresh R (2015) Solution approach to automatic generation control problem using hybridized gravitational search algorithm optimized PID and FOPID controllers. Adv Electr Comput Eng 15(2):23–34
17. Ersdal AM, Imsland L, Uhlen K (2016) Model predictive load-frequency control. IEEE Trans Power Syst 31(1):777–785
18. Arya Yogendra (2019) AGC of restructured multi-area multi-source hydrothermal power systems incorporating energy storage units via optimal fractional-order fuzzy PID controller. Neural Comput Appl 31:851–872
19. Dahiya P, Sharma V, Naresh R (2016) Automatic generation control using disrupted oppositional based gravitational search

algorithm optimized sliding mode controller under deregulated environment. IET Gener Transm Distrib 10(16):3995–4005
20. Abd-Elazim SM, Ali ES (2018) Load frequency controller design of a two-area system composing of a PV grid and a thermal generator via firefly algorithm. Neural Comput Appl 30:607–616
21. Seyedali Mirjalili, Mohammad Mirjalili Seyed, Andrew Lewis (2014) Grey wolf optimizer. Adv Eng Softw 69:46–61
22. Faris Hossam, Aljarah Ibrahim, Al-Betar Mohammed Azmi, Mirjalili Seyedali (2018) Grey wolf optimizer: a review of recent variants and applications. Neural Comput Appl 30:413–435
23. Seyedali Mirjalili (2015) The ant lion optimizer. Adv Eng Softw 83:80–98
24. Patel Nimai Charan, Sahu Binod Kumar, Bagarty Durgesh Prasad, Das Pranati, Debnath Manoj Kumar (2019) A novel application of ALO -based fractional order fuzzy PID controller for AGC of power system with diverse sources of generation. Int J Electr Eng 56(3):1–23
25. Mirjalili S, Lewis A (2016) The whale optimization algorithm. Adv Eng Softw 95:51–67
26. Saremi Shahrzad, Mirjalili Seyedali, Lewis Andrew (2017) Grasshopper optimisation algorithm: theory and application. Adv Eng Softw 105:30–47
27. Mirjalili Seyedali, Gandomi Amir H, Mirjalili Seyedeh Zahra, Saremi Shahrzad, Faris Hossam, Mirjalili Seyed Mohammad (2017) Salp swarm algorithm: a bio-inspired optimizer for engineering design problems. Adv Eng Softw 114:163–191
28. El Hadi Abdulbaset, Saad Zuomin Dong, Karimi Meysam (2017) A comparative study on recently-introduced nature-based global optimization methods in complex mechanical system design. Algorithms 10(4):120
29. Abido MA (2002) Optimal design of power-system stabilizers using particle swarm optimization. IEEE Trans Energy Convers 17(3):406–413
30. Yang XS, Gandomi Hossein (2012) A. Bat algorithm: a novel approach for global engineering optimization. Eng Comput 29:464–483
31. Muro C, Escobedo R, Spector L, Coppinger R (2011) Wolf-pack (Canis lupus) hunting strategies emerge from simple rules in computational simulations. Behav Process 88:192–197
32. Mohamed TH, Bevrani H, Hassan AA, Hiyama T (2011) Decentralized model predictive based load frequency control in an interconnected power system. Energy Convers Manag 52:1208–1214
33. Marwaha S, Lather JS, Dhillon SS (2015) Multi area load frequency control using model predictive controller. In: International conference on electrical and electronics engineering, pp 317–323
34. Liu X, Nong H, Xi K, Yao X (2013) Robust distributed model predictive load frequency control of interconnected power system. Math Prob Eng 6:1–10
35. Singh Amita, Sharma Veena, Dahiya Preeti, Sharma Ram N (2018) Model predictive based load frequency control of interconnected power systems. Recent Adv Electr Electr Eng 11(3):322–333